Meteoritics & Planetary Science 42, Nr 4/5, 655–666 (2007)
Abstract available online at http://meteoritics.org

Hydrothermal alteration in the Bosumtwi impact structure: Evidence from $2M_1$-muscovite, alteration veins, and fracture fillings

Michael T. PETERSEN[1*], Horton E. NEWSOM[1], Melissa J. NELSON[1], and Duane M. MOORE[2]

[1]Institute of Meteoritics, University of New Mexico, Albuquerque, New Mexico 87131, USA
[2]Department of Earth and Planetary Sciences, University of New Mexico, Albuquerque, New Mexico 87131, USA
[*]Corresponding author. E-mail: mikepet@unm.edu

(Received 17 October 2006; revision accepted 20 February 2007)

Abstract–Drill-core samples from the Bosumtwi impact structure (1.07 Myr old and 10.5 km in diameter) in Ghana exhibit mineralogical evidence for post-impact hydrothermal alteration. Nine samples of drill core obtained through the 2004 International Continental Scientific Drilling Project (ICDP) were studied, including an uppermost fallback layer overlying impactite breccias, and partly deformed massive meta-graywacke bedrock. The petrographic study revealed alteration veins containing secondary sericitic muscovite (comparable to $2M_1$-muscovite) crosscutting original bedding in meta-graywacke and forming a matrix between clasts in impactite breccias. X-ray diffraction (XRD) shows that these impactite samples are rich in $2M_1$-muscovite, consistent with post-impact fluid deposition and alteration. Optical analysis indicates the presence of a pre-impact stratiform chlorite in meta-graywacke samples and a secondary alteration chlorite occurring in all samples. Secondary illite was detected in upper impactites of drill core LB-08A and samples containing accretionary lapilli. The lower temperature constraint for the hydrothermal event is given by $2M_1$-muscovite, secondary chlorite, and illite, all of which form at temperatures greater than 280 °C. An absence of recrystallization of quartz and feldspar indicates an upper temperature constraint below 900 °C. The presence of alteration materials associated with fractures and veins in the uppermost impactites of drill cores LB-07A and LB-08A indicates that a post-impact hydrothermal system was present in and adjacent to the central uplift portion of the Bosumtwi impact structure. A sample containing accretionary lapilli obtained from drill core LB-05A exhibits limited evidence that hydrothermal processes were more widespread within the impactites on the crater floor.

INTRODUCTION

The Bosumtwi impact structure is located in Ghana, Africa, and is centered at 6°30′′N, 1°25′′W. Once thought of as a volcanic caldera (Junner 1937), a number of geochemical tests and the presence of planar deformation features (e.g., Koeberl 1994b; Koeberl and Reimold 2005; Schnetzler et al. 1966, 1967) have confirmed that the crater is an impact structure. The crater has a complex form with a slightly pronounced outer ring 20 km in diameter surrounding the crater rim, which is 10.5 km in diameter, and with a central uplift 1.5 km in diameter (Koeberl et al. 2005). Sediments from Lake Bosumtwi, which is 8.5 km in diameter, cover the central uplift. Koeberl et al. (1997) dated the impact at 1.07 ± 0.05 Myr, using $^{40}Ar/^{39}Ar$ step-heating and fission track methods. From July to October 2004, the International Continental Scientific Drilling Program (ICDP) drilled beneath Lake Bosumtwi to recover lake sediments for paleoclimate studies, and to sample impactites and basement from the central uplift (LB-08A) and from the moat surrounding the central uplift (LB-07A) (Koeberl and Reimold 2005). The following drill-core samples were analyzed in this study to investigate evidence of hydrothermal alteration in the impactites and basement of the crater: samples from drill core LB-07A include polymict lithic breccias B711 (334 m depth) and B797 (348 m depth), and phyllite sample B75241 (473 m depth) from a zone identified as shale, phyllite, and schist (Coney et al. 2007) (Fig. 1). Materials found in drill core LB-08A are similar to materials found in drill core LB-07A. Samples from drill core LB-08A include polymict lithic impact breccias B811 (236 m in depth), B81313 (257 m in depth), and meta-graywacke sample B862624 (373 m in depth) (Ferrière et al. 2007) (Fig. 1). Samples of the 30 cm thick fallback layer containing

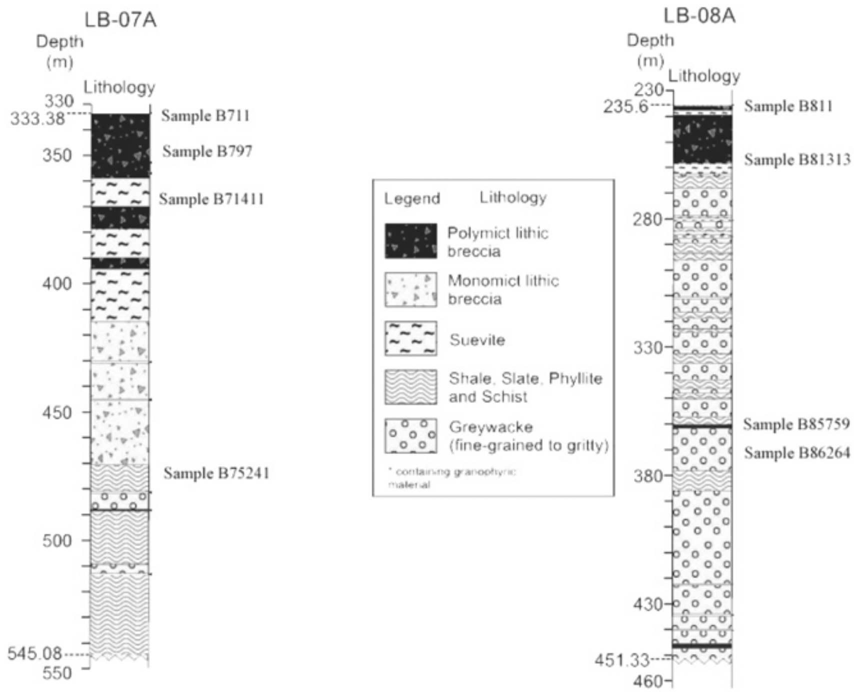

Fig. 1. Stratigraphic column of drill cores LB-07A and LB-08A. Drill core LB-07A was taken from the moat structure surrounding of the central uplift. Drill core LB-08A was taken from the central uplift. Samples analyzed in this study are marked at appropriate depths. Based on Coney et al. (2007) and Ferrière et al. (2007).

accretionary lapilli, LB-05A2 (5–15 cm below sediment base) (Koeberl et al. 2007a) and LB-05A3 (15–30 cm below sediment base), were also studied.

Geological Setting of the Bosumtwi Impact Structure

The Bosumtwi impact structure was emplaced into the lower greenschist facies Ashanti Belt metasediments of the 2.1–2.2 Gyr old Birimian Supergroup (Leube et al. 1990; Koeberl et al. 1998; Koeberl and Reimold 2005; Karikari et al. 2007). The region was intruded by a number of 2.0–2.1 Gyr old granitoid intrusions (Taylor et al. 1992). A variety of lithologies including meta-graywacke, phyllite, quartzite, sandstone, schist, and shale make up the Birimian Supergroup rocks in the region of the crater structure (Koeberl and Reimold 2005; Karikari et al. 2007).

Hydrothermal Alteration

Hydrothermal processes have been documented in many large terrestrial impact structures, such as Sudbury, Ries, Manson, and various impact structures in Russia and Estonia (e.g., Newsom et al. 1986; Ames et al. 1998; McCarville and Crossey 1996; Naumov 2002). Hydrothermal alteration caused by these processes in terrestrial impact structures occurs in association with the impact-melt deposits on the crater floor, at the crater rim, in the central uplift, and in the shocked basement adjacent to the crater fill (Newsom et al. 2001). Hydrothermal processes have recently been documented also in small craters, for example, the Kärdla crater, which is 4 km in diameter (Kirsimae et al. 2002; Puura et al. 2004). The Lonar crater, which is 1.8 km in diameter, may be the smallest crater to have thus far provided evidence of post-impact hydrothermal alteration in basement rocks beneath the crater floor (Hagerty and Newsom 2003). Based on the size of the Bosumtwi impact structure, which is 10.5 km in diameter, evidence of hydrothermal processes associated with the impact were expected to be present in samples from the crater floor and central uplift (Koeberl 1994a).

METHODS

Sampling

The majority of the samples examined in this study are from drill cores LB-07A and LB-08A obtained by the Lake Bosumtwi Drilling Project (Koeberl et al. 2007b). Drill cores LB-07A and LB-08A were taken to sample the impactite deposits and the target rocks. The approximate depths and lithologies of samples analyzed in this study are shown in the stratigraphic profiles of Fig. 1. In addition, C. Koeberl provided material containing accretionary lapilli from the upper 30 cm of the fallback layer located in between polymict lithic breccia and lake sediment at the base of sediment drill core LB-05A (Koeberl et al. 2007a).

Table 1. Electron microprobe analyses of mineral grains including phyllosilicates in polymict lithic breccia sample B797 (348 m depth) from drill core LB-07A (Fig. 4). Dark phase analysis is an illite composition. The light phase analyses are chlorite compositions.

Sample	SiO_2 (wt%)	Al_2O_3 (wt%)	FeO (wt%)	MgO (wt%)	CaO (wt%)	K_2O (wt%)	Na_2O (wt%)	Total wt%
LB-07A: dark phase								
B797A-7	44	27	8.8	3.3	0.27	5.75	1.34	90
LB-07A: light phase								
B797A-2	26	23	27	13	0.06	0.04	0.03	89
B797A-3	26	23	27	13	0.05	0.03	0.04	89
Reference compositions								
Illite[a]	50	24	6.5	3.4	0.75	5.8	0.30	91
Muscovite[b]	47	38	0.08	nd	nd	8.9	0.52	95
Chlorite[a]	28	18	21	19	0.19	0.06	0.04	86

[a]Typical illite and chlorite reference compositions from Deer et al. (1966).
[b]Typical muscovite reference compositions from Ahn and Buseck (1998).
nd = none detected.

Experimental Methods: SEM, EMPA, X-ray Diffraction

Polished thin sections were analyzed using optical microscopy, scanning electron microscopy (SEM), and electron microprobe analysis (EMPA) to determine petrographic relationships and geochemical characteristics. Analytical data were collected using the JEOL 8200 automated electron microprobe at the Institute of Meteoritics, Albuquerque, New Mexico. Operating conditions were an accelerating voltage of 15 keV with a spot size of 10 μm and a filament current of 2×10^{-8} nA. Detection limits were <250 ppm for major elements. Mineral calibration standards were orthoclase (Al_2O_3, SiO_2, K_2O), albite (NaO), diopside (MgO, CaO), and olivine (FeO). Totals for EMP analyses that include hydrous minerals are less than 100% and can range from 86 wt% to 95 wt% for typical examples of the hydrous phases observed in this study (e.g., Table 1). Totals for nonhydrous silicates, including quartz and feldspar, ranging from 98 to 103 wt% were considered within the analytical uncertainty for the fine grained materials under investigation.

Phyllosilicates were separated from the drill-core samples using the method of Drever (1973) and the <2 μm size fraction was analyzed by X-ray diffraction (XRD). Powdered samples were analyzed in the Department of Earth and Planetary Sciences at the University of New Mexico, using a Scintag Pad V diffractometer with DataScan 4 software from Materials Data Inc. (MDI) for system automation and data collection. Cu-K radiation (40 kV, 35 mA) was used with a Bicron Scintillation detector (with a curved pyrolitic graphite curved crystal monochromator). Data were analyzed with the Jade 6.5 software from MDI using the International Center for Diffraction Data PDF2 database (rev. 2004) for XRD phase identification.

The <2 μm separation procedure began by adding distilled water to each 10 g sample. The samples were then sonicated and centrifuged at 750 rpm for 3.5 min to isolate the <2 μm fraction. This fraction was rinsed until dispersion was achieved. The dispersed <2 μm grains were then vacuumed through 20 μm membranes. The resulting film was pressed onto a glass slide, separating it from the membrane. The sample was allowed to dry before an XRD scan was collected over the 2θ range from 2° to 35°, with 0.05° step intervals, and a dwell time of 4 s. Samples were glycolated after the initial run to determine whether the samples contained any swelling phyllosilicates. Phyllosilicate nomenclature and identification methods are summarized in Moore and Reynolds (1997).

RESULTS

Macroscopic evidence of hydrothermal processes throughout the drill cores was very limited. One of us, Horton Newsom, visually observed submillimeter-scale fractures in the upper and middle portions of drill core LB-08A during drill-core sampling (ICDP). Due to the friable nature of drill core samples, the characteristics and distribution of crosscutting fractures and fracture fillings were most obvious immediately following drill core barrel discharge on the drilling platform before the samples were subsequently boxed and processed. On-site and petrographic observations indicate that fractures in the upper portions of both drill cores, especially LB-08A, are filled by sericitic muscovite, secondary chlorite, and illite. Fractures in the deeper parts of both drill cores tend to be open, and exhibit very limited alteration and leaching effects. We observed no alteration materials (e.g., Fig. 2) in fractures below a depth of 350 m in drill core LB-07A and a depth of 280 m in drill core LB-08A. The detailed results are discussed below for the three main types of materials in the drill cores: the meta-graywacke that makes up a portion of the altered uppermost country rock, the impactites (polymict lithic breccia and suevite) in the upper parts of the drill cores, and samples containing accretionary lapilli from the uppermost fallback layer just below the lake sediment.

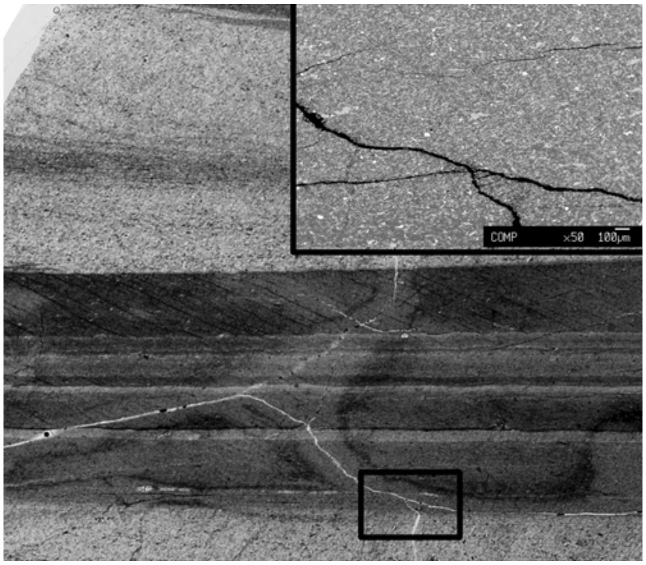

Fig. 2. An optical image (15 mm in width) of a portion of the thin section of meta-graywacke sample B86264 (373 m depth) from drill core LB-08A. Backscattered electron (BSE) image of the portion of the fracture outlined at the bottom of the optical image is shown as an inset (upper right-hand corner). These images show typical meta-graywacke basement material containing phyllosilicates in subhorizontal bedding, crosscut by fractures. The largely empty fractures in the rock are surrounded by a leached zone (not visible in the BSE image) out to 0.5 mm, suggesting mild fluid alteration and chemical transport.

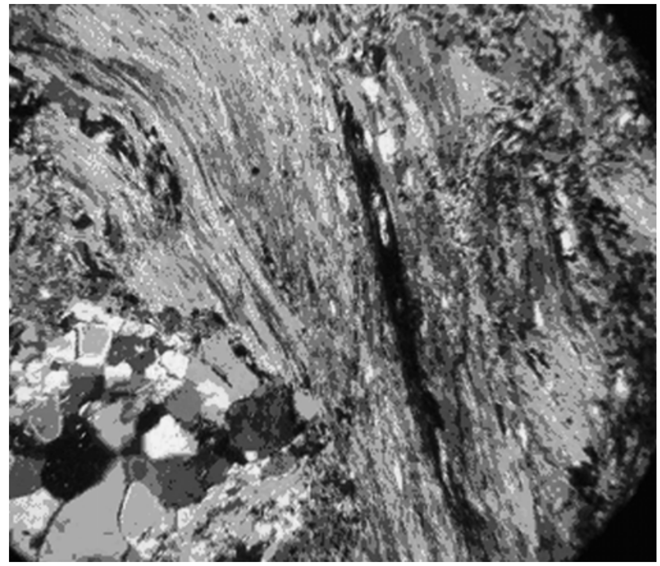

Fig. 3. An optical image (1 mm in width) of a portion of the thin section of polymict lithic breccia sample B797 (348 m depth) from drill core LB-07A. Crossing the center of the image is a vein of muscovite (sericite), exhibiting foliated texture surrounding breccia clasts.

Meta-graywacke

Sample B86264 is from the lower meta-graywacke bedrock units below the impactites in drill core LB-08A, from a depth of 373 m. This sample did not experience significant brecciation or alteration, and does not contain veins with abundant secondary alteration phyllosilicates, though open fractures exist. Thin section observations, confirmed by EMPA, reveal chlorite of probable pre-impact origin oriented parallel to bedding marked especially by quartz and feldspar (Fig. 2). In thin section, most alteration veins are no more than 1 mm across. The mostly empty fractures in the meta-graywacke are found to contain some limited alteration material along the fractures (possibly chlorite). In the lower parts of the drill cores, the open fractures are observed to have leaching halos that do not extend for more than 1 mm from a fracture, suggesting the presence of fluids at one time (Fig. 2). Surprisingly the EMP analyses for major elements (not listed) showed no variations across the leached zone.

Impactites (Polymict Lithic Breccia and Suevite)

Petrography

Sample B711 is from the polymict lithic breccia in drill core LB-07A at a depth of 334 m (Fig. 1). It is composed of brecciated graphitic schist, meta-graywacke, and shocked quartz which displays both undulatory and mosaic extinction. There is a greenish alteration throughout the thin section, suggesting secondary chlorite formation. Sample B797 from 348 m depth in drill core LB-07A contains a clast of graphitic schist, which has been fractured and brecciated, presumably by the impact event. The observed graphitic schist band is 2 mm thick and extends completely through the drill core. The fragments of graphitic schist are surrounded by sericitic muscovite. The sericitic muscovite and opaque minerals have a foliated texture aligned with the edges of the apparent vein or fracture orientations and wrap around the edges of clasts (Fig. 3). A brecciated portion of the sample was analyzed by EMP and consists of fragments of secondary chlorite and illite phyllosilicates (Table 1; Fig. 4).

Sample B811 was obtained from 236 m depth from the interval described as the uppermost polymict lithic breccia occurrence in drill core LB-08A (Ferrière et al. 2007). Our sample is not a lithic clast, but represents a glassy vesicular impact-melt fragment with chlorite alteration marked by a greenish tinge in thin section, as well as illite composition phases (Fig. 5; Table 3). Polymict lithic breccia sample B81313 from 257 m depth is composed of shocked quartz, secondary chlorite, opaque minerals, and sericitic muscovite demonstrating the same foliated texture described in sample B797 above (Fig. 6; Table 4).

EMP and SEM Analysis

EMP analyses of alteration vein fillings found in samples B711, B799, B811, and B81313 reveal chlorite and illite compositions. Backscattered electron (BSE) images and

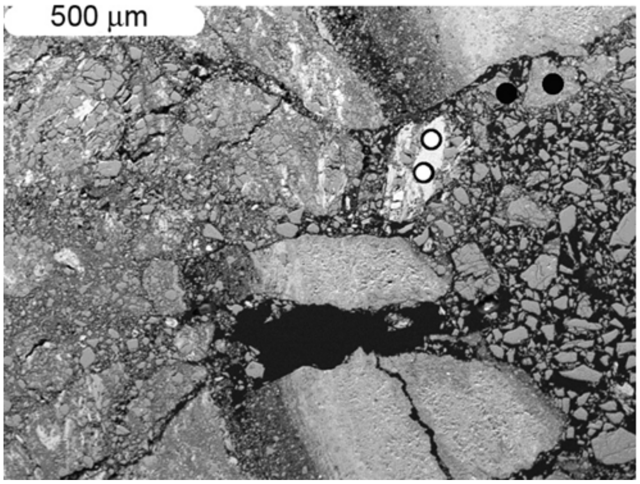

Fig. 4. A BSE image of polymict lithic breccia portion of sample B797 (348 m depth) from drill core LB-07A. Light-colored clasts in the center of the image are composed of illite; dark dots indicate fragments of fine-grained basement with predominantly chlorite composition. The sample is fractured due to syn-impact or post-impact processes. Data for the indicated points are presented in Table 1.

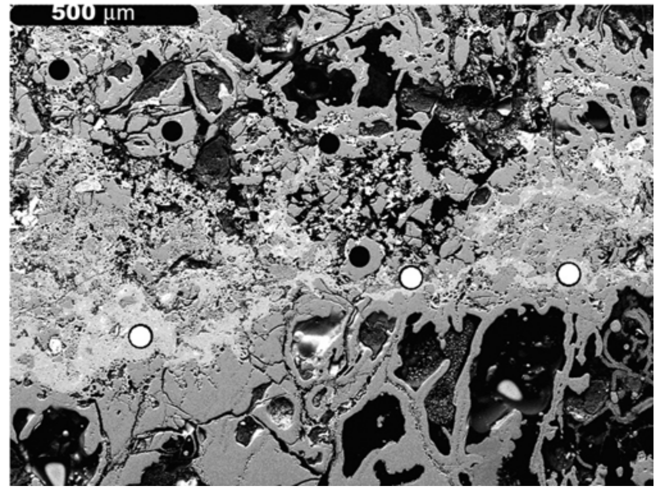

Fig. 5. A BSE image of polymict lithic breccia sample B811 from 236 m depth from drill core LB-08A. Vesicular melt texture is observed in the lower portion of the image, juxtaposed with an alteration vein resembling a light-colored zone running subhorizontally through the thin section. Points represent locations of EMP analyses reported in Table 3, where the open circles represent "light phase" analyses.

optical microscopy reveal stratiform and secondary alteration forms of chlorite. Quantitative EMP element maps of the rims of breccia fragments in sample B811 reveal magnesium enrichment compared to the clast centers of up to a concentration of 3 wt%, enriched aluminum abundances up to a concentration of 10 wt%, and accompanying depletion of silicon abundances down to a concentration of 10 wt% (Fig. 7). Sample B811 contains silica-rich vesicular melt clasts juxtaposed with areas containing illite veins (Table 3; Fig. 5). Electron microprobe analyses of sample B81313 reveal compositions corresponding to illite, a diagenetic material after muscovite (Fig. 6; Table 4).

X-ray Diffraction

XRD analysis was used to confirm that $2M_1$-muscovite and at least two chlorite structures were present in several samples from both drill cores, as had been previously suggested by our optical microscopy work (see Table 2). XRD patterns confirmed the presence of chlorite-rich phyllosilicates in all samples analyzed from both drill cores, as well as $2M_1$-muscovite from the impactites (Figs. 8 and 9). The XRD pattern that defines $2M_1$-muscovite is marked by "stair-step down" peaks at 2θ values of 30.0°, 31.3°, and 32.1° with relative intensities of 35, 30, and 25 (Fig. 10) (Moore and Reynolds 1997).

Table 2. Results of X-ray diffraction analyses of <2 μm size particles in samples from drill cores LB-07A and LB-08A.

Sample	Depth from lake level (m)	$2M_1$ muscovite	Chlorite
LB-07A			
B711	334	Present	Present
B797	348	Present	Present
B71411	356	Present	Present
B75241	473	nd	Present
LB-08A			
B811	236	Present	Present
B81313	257	Present	Present
B86264	373	nd	Present

nd = none detected.

Accretionary Lapilli–Containing Samples

Petrography

Samples LB-05A2 and LB-05A3 are composed of subspherical accumulations of fine clastic material (accretionary lapilli) up to 2 mm in diameter, microtektite-like glass spherules, quartz, and shocked quartz (Koeberl et al. 2007a) (Fig. 11). BSE images revealed random textural orientations of fine clastic material (Figs. 11 and 12). Three lapilli of 0.5 to 1 mm diameters have a fine clastic matrix with angular target rock particles up to 200 μm in size, giving the appearance of dust-sized mineral fragments. Electron microprobe element mapping of the lapilli matrix reveals discrete elemental compositions of the mineral fragments (Fig. 12). However, some local areas show the presence of alteration phases associated with fractures and matrix between larger breccia fragments and accretionary lapilli. In one example, the alteration is present in the form of a dark rind on a vesicular clast adjacent to the fracture, and as fibrous-textured matrix material (Fig. 13; Table 5).

Table 3. Electron microprobe analyses of phyllosilicates of illite composition in a vein adjacent to a vesicular melt clast from polymict lithic breccia sample B811 (236 m depth) from drill core LB-08A (Fig. 5).

Sample	SiO_2 (wt%)	Al_2O_3 (wt%)	FeO (wt%)	MgO (wt%)	CaO (wt%)	K_2O (wt%)	Na_2O (wt%)	Total wt%
LB-08A: light phase								
B811B-1	44	30	6.3	2.8	2.9	4.6	0.87	92
B811B-6	46	29	7.2	3.4	4.2	4.3	0.76	95
B811B-7	47	28	6.0	2.8	2.9	4.2	1.3	92

nd = none detected.

Table 4. Electron microprobe analyses of phyllosilicates of illite and chlorite compositions in an alteration vein in polymict lithic breccia sample B81313 (257 m depth) from drill core LB-08A (Fig. 6).

Sample	SiO_2 (wt%)	Al_2O_3 (wt%)	FeO (wt%)	MgO (wt%)	CaO (wt%)	K_2O (wt%)	Na_2O (wt%)	Total wt%
LB-08A: light phase								
B81313C-8	25	23	29	10	0.16	0.11	0.06	88
B81313C-9	38	27	7.1	2.7	0.12	5.3	0.51	81
B81313C-11	24	24	29	11	0.08	0.05	nd	88
B81313C-12	24	24	29	10	0.13	0.04	nd	87

nd = none detected.

DISCUSSION

A rather surprising result of the drill core stratigraphy is the fact that a thinner suite of impactites was encountered than expected based on the earlier geophysical studies (e.g., Scholz et al. 2002). The results of the initial evaluation of the stratigraphy of the drill cores (Coney et al. 2007; Ferrière et al. 2007) show that only 45 m of impact-melt–bearing deposits are present in drill core LB-07A, and 20 m in drill core LB-08A. The extent of hydrothermal alteration became of considerable importance in view of the relatively thin sheet of impact melt in these drill cores. Evidence of hydrothermal alteration in other impact structures includes altered impact breccias and evidence of deposition of secondary minerals due to fluid transport along fractures (Naumov 2002; Newsom et al. 1986). In the Bosumtwi samples that we have analyzed, analogous features have been observed including breccias with an altered matrix and deposition of secondary alteration minerals due to fluid transport along fractures.

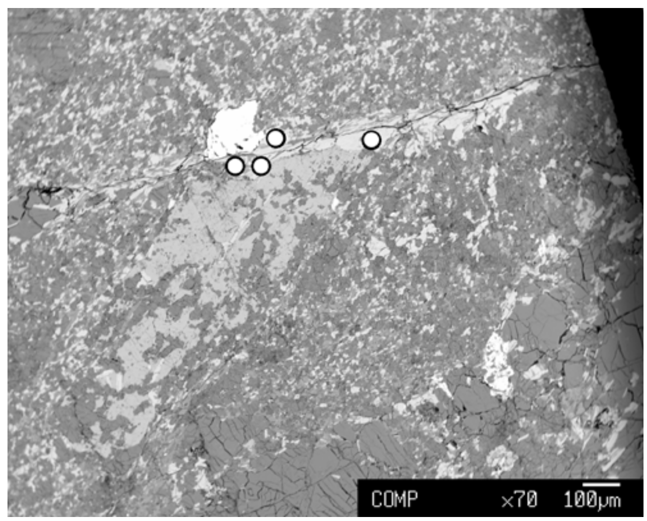

Fig. 6. A BSE image of polymict lithic breccia sample B81313 from 257 m depth from drill core LB-08A, containing a crosscutting alteration vein. Electron microprobe analyses are marked by open circles for chlorite. These analyses are reported in Table 4.

Pre-Impact Phases versus Post-Impact Phases

One significant purpose of this study was to determine the paragenesis of alteration phases relative to the impact event. The presence of fracture-filling material in the upper portions of the drill cores and observations of non-filled fractures at greater depth shed light on the pre-impact and post-impact origin of individual phases. It is highly unlikely that fracture-filling materials were formed during the greenschist facies metamorphism event; otherwise they would not be so well constrained to the impactites. Chlorites in the drill cores were formed due to early greenschist facies metamorphism and in later, possibly impact-related hydrothermal processes. The subparallel to bedding characteristics of the stratiform chlorites in the meta-graywacke are presumed to be due to early (2.0–2.1 Gyr) metamorphism. The secondary chlorite fracture fillings are assumed to be related to post-impact hydrothermal processes. Although McCarville and Crossey (1996) noted that chlorite-rich phyllosilicates in the Manson impact structure in Iowa were formed at temperatures above 300 °C, Walker (1987, 1993) determined that chlorite-rich alteration minerals are very capable of forming at temperatures well below 200 °C.

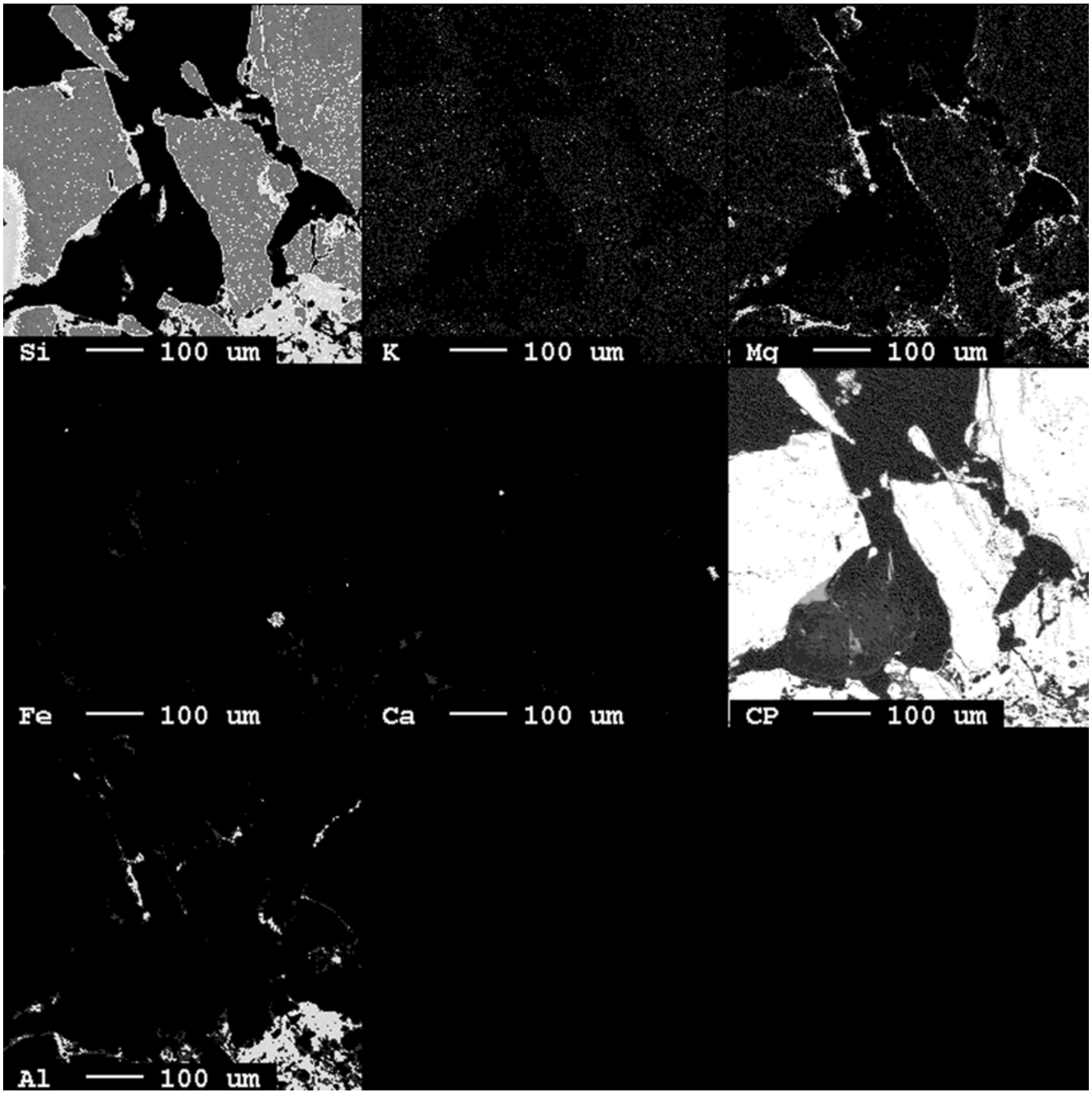

Fig. 7. Black-and-white semi-quantitative versions of quantitative element maps for a section of polymict lithic breccia sample B811 from a depth of 236 m from drill core LB-08A. The area shown is from the contact between breccia and melt clasts, with breccia clasts denoted by lighter colors in "CP" cell. The "CP" cell displays BSE image. The rims of breccia clasts have Si concentrations up to 37 wt%, Mg concentrations up to 3 wt%, and Al concentrations up to 10 wt%. In this black and white image, lighter colors indicate higher concentrations.

The presence of illite, $2M_1$-muscovite, and secondary chlorite alteration phases and observations of their textures in fracture fillings and veins support the formation of this material during a late alteration event due to the impact. Foliated textures of fracture fillings rich in sericitic muscovite may be partially due to post-impact deformation of the upper impactites. However, additional work is required on non-impacted basement rocks from far away from the crater to more confidently rule out the formation of these secondary phases during granitoid intrusion and lower greenschist facies metamorphism. The lack of major geologic activity surrounding the impact structure since the 2.0–2.1 Gyr old granitoid intrusions (Taylor et al. 1992) suggests that these alteration phases were formed in response to the impact. Our study suggests that while a post-impact hydrothermal event probably occurred, the effects were largely limited to the impactites, and the extent of alteration was very small.

Evidence of Alteration and Hydrothermal Processes

Evidence for the effects of post-impact hydrothermal fluids was found in several settings:

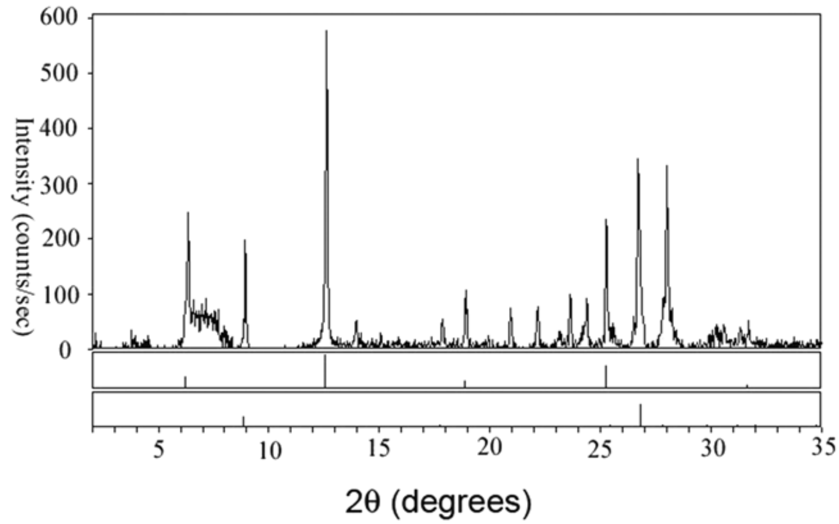

Fig. 8. An X-ray diffraction pattern for polymict breccia sample B811 from 236 m depth from drill core LB-08A, containing both $2M_1$-muscovite and chlorite. Upper peak identification shows relative peak heights and positions for chlorite, lower peak identification shows relative peak heights and positions for $2M_1$-muscovite.

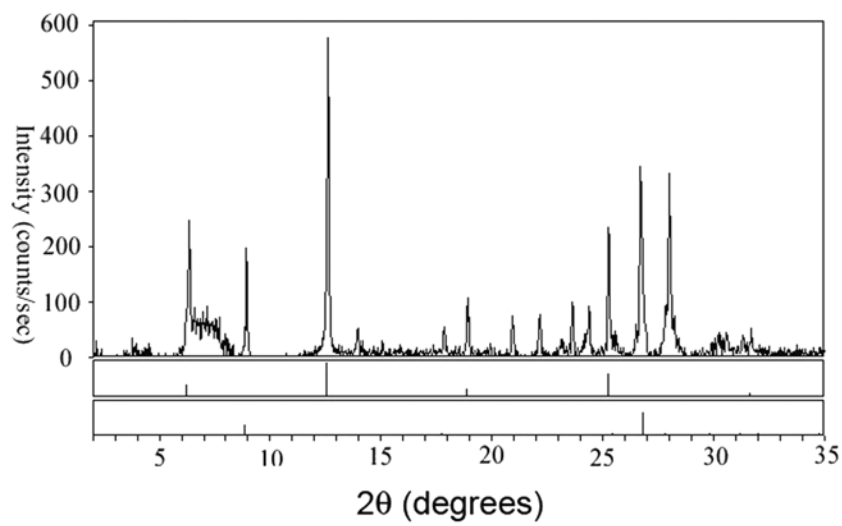

Fig. 9. An X-ray diffraction pattern of polymict lithic breccia sample B81313 from 257 m depth from drill core LB-08A, containing both $2M_1$-muscovite and chlorite. Upper peak identification shows relative peak heights and positions of chlorite, lower peak identification shows relative peak heights and positions for $2M_1$-muscovite.

Fractures and Fracture Fillings

The occurrence of post-impact phyllosilicate-bearing alteration veins and fracture fillings and the XRD evidence for the presence of $2M_1$-muscovite in bulk samples suggests that hydrothermal fluids were produced immediately following the impact. Dewey and Moore (1997) stated that the $2M_1$-muscovite polytype first appears with the lowest temperature metamorphic zone known as the "anchizone," which has a temperature of 280–360 °C. Absence of melt or recrystallization of feldspars and other common minerals places an upper limit for alteration near 900 °C (Deer et al. 1966). Although the basement rocks experienced lower greenschist facies metamorphism that involved similar temperatures, the presence of alteration veins and fracture fillings in the upper portions of drill cores LB-07A and LB-08A and alteration veins crosscutting breccia clasts in the uppermost polymict lithic breccias suggest that the veining and vein-filling events occurred due to the impact. Comparison of the EMP analyses of the sericitic muscovite to EMP analyses of chlorites reveals a greater abundance of magnesium and iron in the secondary chlorite found in fractures crosscutting breccia clasts than in the sericitic muscovite found in similar fractures. This comparison suggests fluid mobilization of magnesium and iron in this system.

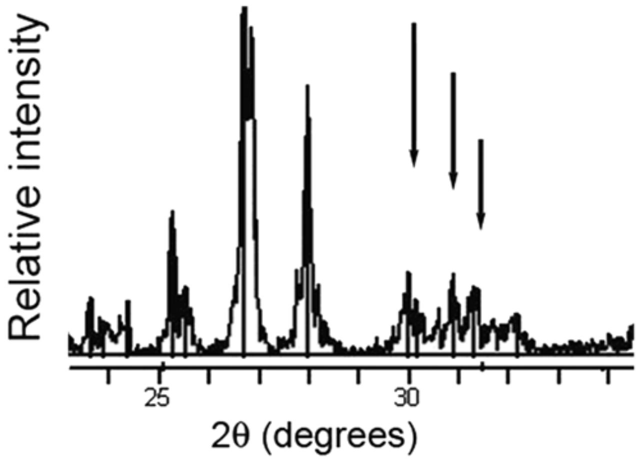

Fig. 10. A close-up of a section of the XRD pattern for polymict lithic breccia sample B797 from a depth of 348 m from drill core LB-07A. Arrows illustrate "stair-step down" pattern for the interval from 30–33°, which is indicative of $2M_1$-muscovite.

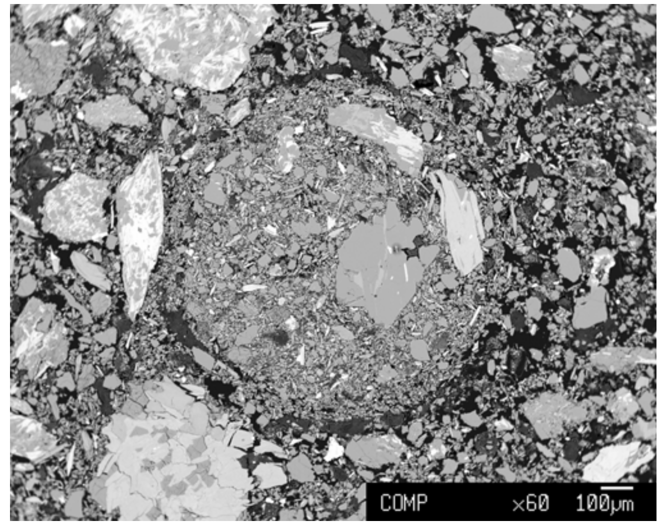

Fig. 11. A BSE image of accretionary lapilli containing sample 117A2 from 117 m depth from drill core LB-05A displaying an example of the accretionary lapilli present in this sample. The spherical aggregate of mineral fragments suggests aggregation in the atmosphere before deposition in the crater (see also Koeberl et al. 2007a).

Samples Containing Accretionary Lapilli

Evidence for hydrothermal activity was observed affecting the samples containing accretionary lapilli. For example, in BSE images (Fig. 13) the alteration consists of rinds and fibrous matrix material adjacent to a fracture, arguing for a post-impact origin. EMP analyses of the matrix also suggest the presence of phases with chlorite chemistry. The limited amount of visible alteration minerals in the BSE images, and the lack of elemental enrichments or depletions on the rims of clasts in the EMP element map suggest that aqueous (possibly hydrothermal) alteration was of limited extent at this location, approximately 1 km southwest of the central uplift. The presence of illite in the samples containing accretionary lapilli is indicative of alteration temperatures greater than 100 °C (Moore and Reynolds 1997).

The presence of aerodynamically shaped accretionary lapilli and melt clasts as the uppermost impactite deposit suggests deposition from a cloud of debris above the crater. Lapilli found in volcanic settings accrete from abundant water and steam in an eruption column, allowing fine-grained materials to coalesce. The resulting eruption produces a cloud analogous to a Plinian eruption or nuclear fireball cloud over the crater (Newsom et al. 1990). Given the previously published evidence for an oblique impact at Bosumtwi (Koeberl and Reimold 2005; Artemieva et al. 2004), the evidence from the accretionary lapilli for a cloud of debris above the crater suggests that atmospheric effects during oblique impacts are similar to the atmospheric effects observed in craters formed by higher-angle impacts.

Comparisons with Other Impact Structures

Naumov et al. (2002) summarized data on hydrothermal alteration in many impact craters. The presence of minerals suggesting hydrothermal alteration at low temperatures (less than 300–350 °C) commonly includes chlorite as found in this study of the Bosumtwi impactites. The presence of sericitic muscovite has been less commonly reported, though it has been observed, for example, at Lac Couture, Mien, Mistastin, and Pilot Lake (all in Canada). The presence of illite was observed as an alteration phase in the Ries impact structure (Newsom et al. 1986).

Our results suggest that the Bosumtwi drill-core samples from LB-07A and LB-08A experienced a very limited but relatively high temperature hydrothermal alteration episode that has similarities to the Manson structure (McCarville and Crossey 1996). In contrast, the samples from the Yaxcopoil-1 drill core from the Chicxulub impact structure in Mexico experienced a greater extent of hydrothermal alteration, but mostly at lower temperatures that did not lead to extensive chlorite or illite formation (Newsom et al. 2006). The nature of the hydrothermal episodes in these craters can be explained by three controlling factors: 1) the target lithology, 2) drilling location and distance to heat source from the impact, and 3) proximity to flooding by sea water in the case of Yaxcopoil-1 (Tuchscherer et al. 2005). The Bosumtwi drill cores and the Manson drill core were obtained from the vicinity of the central uplifts, while the Yaxcopoil-1 core was located outside the transient cavity away from other heat sources.

Implications

Our results are consistent with evidence of an impact event at the Bosumtwi impact structure followed by a relatively high-temperature post-impact hydrothermal alteration event of limited magnitude in the vicinity of the central uplift. Although not diagnostic of impact, the breccias,

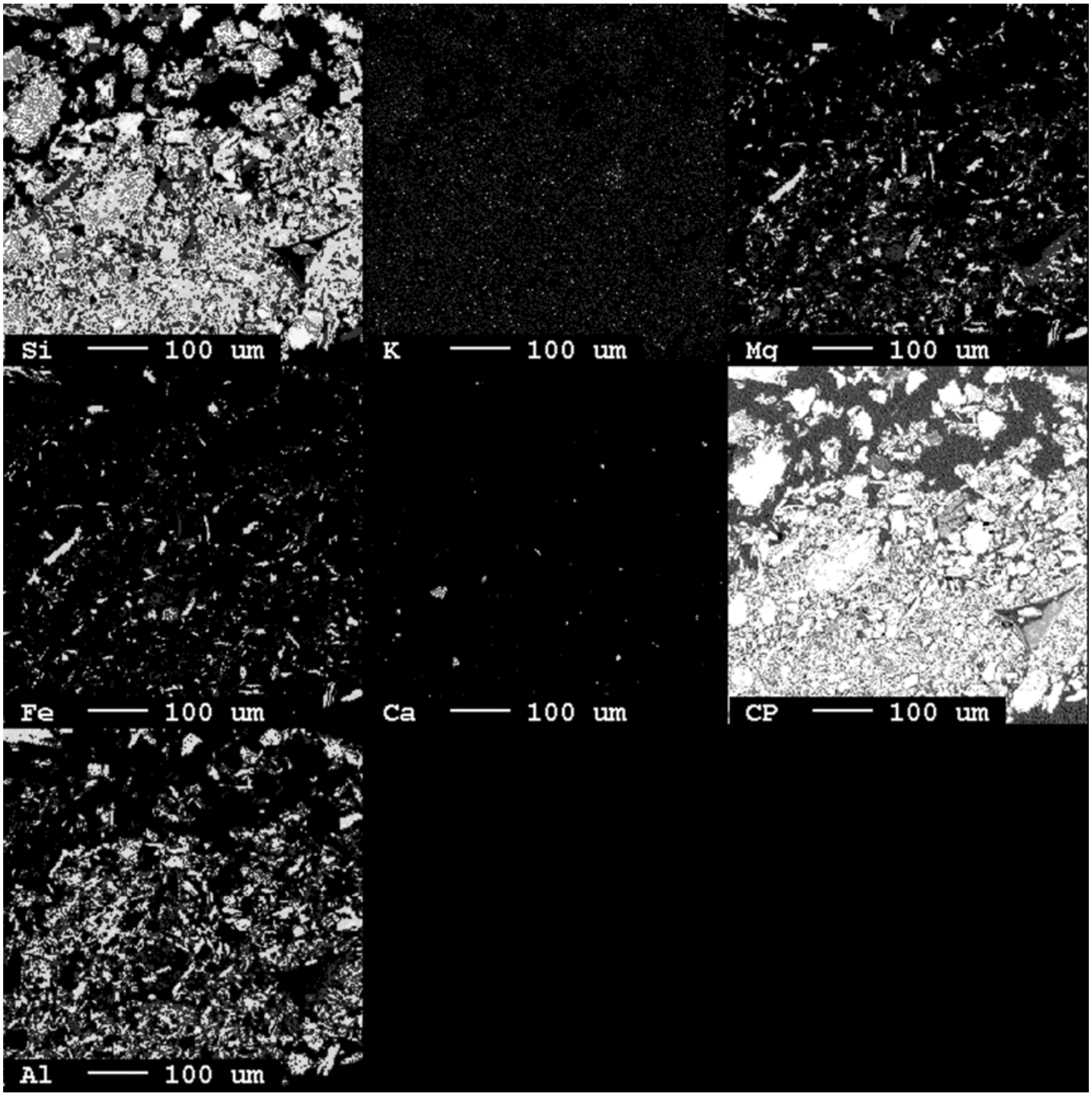

Fig. 12. Black-and-white semi-quantitative versions of quantitative element maps of a portion of accretionary lapilli containing sample 117A2 from a depth of 117 m from drill core LB-05A. The map covers the border between an accretionary lapilli (bottom right) and the groundmass (upper left). The rims of groundmass clasts and accretionary lapilli fragments have Si concentrations up to 85 wt%, Mg concentrations up to 15 wt%, Fe concentrations up to 24 wt%, and Al concentrations up to 30 wt%. In this black and white image, lighter colors indicate higher concentrations. "CP" cell displays BSE image.

Table 5. Electron microprobe analyses of phyllosilicates in an alteration zone adjacent to a fracture between accretionary lapilli particles and a melt clast in sample LB05-A2 (117 m depth) from drill core LB-05A (Fig. 13).

Sample	SiO_2 (wt%)	Al_2O_3 (wt%)	FeO (wt%)	MgO (wt%)	CaO (wt%)	K_2O (wt%)	Na_2O (wt%)	Total wt%
Fallback layer								
LB-05A2B-10	40	8.2	28	4.4	1.8	1.5	0.24	85
LB-05A2B-12	25	21	24	15	1.8	0.02	nd	88
LB-05A2B-14	25	23	25	11	0.04	0.05	nd	84
LB-05A2B-19	43	8.1	27	4.2	1.6	1.3	0.42	86
LB-05A2B-21	26	20	24	15	nd	nd	nd	86

nd = none detected.

fractures, and fracture fillings observed in the Bosumtwi drill cores, on and adjacent to the central uplift, are best explained by processes associated with the formation of the impact structure. The fracture fillings and alteration in the upper portions of the drill cores and leaching of the fracture margins in the lower portions of the drill cores provide evidence for post-impact fluid transport. Evidence for hydrothermal alteration at elevated temperatures comes from the XRD evidence for the presence of the $2M_1$-muscovite and secondary chlorite associated with post-impact fracture fillings.

Considering the size of the Bosumtwi impact structure, the amount of hydrothermal alteration in drill cores LB-07A and LB-08A in the vicinity of the central uplift of the crater is limited in extent. This is consistent with the thinner than expected amount of impactites encountered in the drill cores, compared to the geophysical interpretations (Scholz et al. 2002).

Possible explanations for the low amount of impact melt and hydrothermal alteration are: 1) an oblique impact, where the maximum heat and pressure from the impact was not translated deeply into the Earth's crust (Artemieva et al. 2004; Koeberl and Reimold 2005), and that 2) the supply of water in the vicinity of the central uplift may have been limited to rainwater and hydrous minerals immediately following the impact while substantial heat was present. A limited water supply would also be consistent with the persistence of high temperatures in the impactites long enough to allow the formation of alteration minerals such as secondary chlorite and $2M_1$-muscovite.

CONCLUSIONS

The Bosumtwi impact structure contains evidence for a sequence of syn-impact and post-impact events as follows:

- The presence of impact melt-bearing breccias and fracturing that were observed in both drill cores LB-07A and LB-08A are consistent, yet not necessarily diagnostic, of an impact event.
- Brecciated fragments are commonly surrounded by phyllosilicate alteration veins.
- The fracture fillings in the upper drill-core samples are consistent with post-impact fluid deposition and alteration, due to crosscutting relationships between alteration veins and impactites, as well as the different compositions of the phyllosilicates found along these crosscutting veins.
- The presence of $2M_1$-muscovite and its physical relationships with the surrounding rocks exhibits evidence of low to moderate temperature hydrothermal alteration.
- The material containing accretionary lapilli gives evidence for a debris cloud, which rose above the crater after impact. This observation provides constraints on the atmospheric effects during an oblique impact.

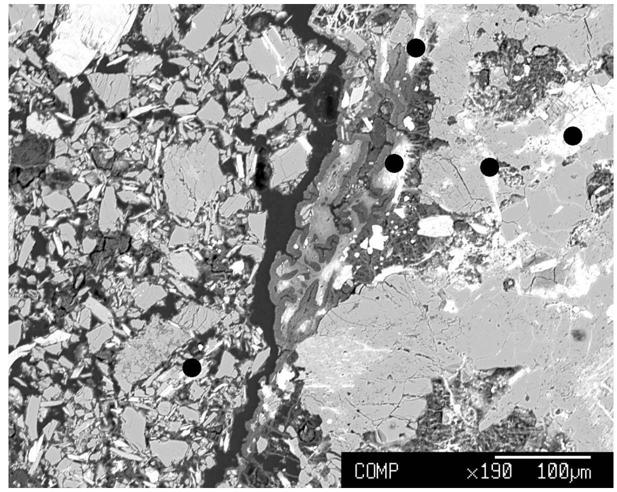

Fig. 13. A BSE image of sample 117A2 (117 m depth) in drill core LB05-A. A vertically oriented open fracture (filled with epoxy) is present between a clast on the right and accretionary mineral matrix material on the left. Alteration is present in the form of a dark rind on a vesicular clast adjacent to the fracture, and as fibrous-textured matrix material in the clast to the right. EMP analyses of the locations indicated by filled circles are reported in Table 5.

Acknowledgments–Drilling at Bosumtwi was supported by the International Continental Drilling Program (ICDP), the U.S. NSF-Earth System History Program under grant no. ATM-0402010, Austrian FWF (project P17194-N10), the Austrian Academy of Sciences, and by the Canadian NSERC. Drilling operations were performed by DOSECC. Thanks to Jim Connolly for assistance with XRD. We thank C. Koeberl for directing the deep drill core sampling part of the project, and for facilitating the participation of H. N. in the field operations. We wish to thank R. T. Schmitt, W. U. Reimold, and an anonymous reviewer for extremely helpful reviews. We are very grateful to W. U. Reimold and C. Koeberl who were extremely generous with their extensive reviews and patience during the final stages of preparation of this manuscript. Research supported by NASA Planetary Geology and Geophysics program grant NAG 5-11496 and supplements.

Editorial Handling—Dr. Wolf Uwe Reimold

REFERENCES

Ahn J. H. and Buseck P. R. 1998. Transmission electron microscopy of muscovite alteration of tourmaline. *American Mineralogist* 83:535–541.

Ames D. E., Watkinson D. H., and Parrish R. R. 1998. Dating of a regional hydrothermal system induced by the 1850 Ma Sudbury impact event. *Geology* 26:447–450.

Artemieva N. A., Karp T., and Milkereit B. 2004. Investigating the Lake Bosumtwi impact structure: Insight from numerical modeling. *Geochemistry Geophysics Geosystems* 5, doi:10.1029/2004GC000733.

Coney L., Reimold W. U., Gibson R. L., and Koeberl C. 2007. Geochemistry of impactites and basement lithologies from ICDP borehole LB-07A, Bosumtwi impact structure, Ghana. *Meteoritics & Planetary Science* 42. This issue.

Deer W. A., Howie R. A., Zussman J. 1966. *An introduction to the rock-forming minerals*. London: William Clowes & Sons Limited. 528 p.

Drever J. I. 1973. The preparation of oriented clay mineral specimens for X-ray diffraction analysis by a filter-membrane peal technique. *American Mineralogist* 58:553–554.

Ferrière L., Koeberl C., Reimold W. U., and Mader D. 2007. Drill core LB-08A, Bosumtwi impact structure, Ghana: Geochemistry of fallback breccia and basement samples from the central uplift. *Meteoritics & Planetary Science* 42. This issue.

Hagerty J. J. and Newsom H. E. 2003. Hydrothermal alteration at the Lonar Lake impact structure, India: Implications for impact cratering on Mars. *Meteoritics & Planetary Science* 38:365–381.

Junner N. R. 1937. The geology of the Bosumtwi caldera and surrounding country. *Gold Coast Geological Survey and Bulletin* 8:1–38.

Karikari F., Ferrière L., Koeberl C., Reimold W. U., and Mader D. Petrography, geochemistry, and alteration of country rocks from the Bosumtwi impact structure, Ghana. *Meteoritics & Planetary Science* 42. This issue.

Kirsimae K., Suuroja S., Kirs J., Karki A., Polikarpus M., Puura V., and Suuroja K. 2002. Hornblende alteration and fluid inclusions in Kärdla impact crater, Estonia: Evidence for impact-induced hydrothermal activity. *Meteoritics & Planetary Science* 37:449–457.

Koeberl C. 1994a. African meteorite impact craters: Characteristics and geological importance. *Journal of African Earth Science* 18: 263–295.

Koeberl C. 1994b. Tektite origin by hypervelocity asteroidal or cometary impact: Target rocks, source craters, and mechanisms. In *Large meteorite impacts and planetary evolution*, edited by Dressler B. O., Grieve R. A. F., and Sharpton V. L. GSA Special Paper #293. Boulder, Colorado: Geological Society of America. pp. 133–151.

Koeberl C. and Reimold W. U. 2005. Bosumtwi impact crater, Ghana (West Africa): An updated and revised geological map, with explanations. *Jahrbuch der Geologischen Bundesanstalt, Wien* (*Yearbook of the Austrian Geological Survey*) 145:31–70 (+1 map, 1:50,000).

Koeberl C., Bottomley R. J., Glass B. P., and Storzer D. 1997. Geochemistry and age of the Ivory Coast tektites and microtektites. *Geochimica et Cosmochimica Acta* 61:1745–1722.

Koeberl C., Reimold W. U., Blum J. D., and Chamberlain C. P. 1998. Petrology and geochemistry of target rocks from the Bosumtwi impact structure, Ghana, and comparison with Ivory Coast tektites. *Geochimica et Cosmochimica Acta* 62:2179–2196.

Koeberl C., Brandstätter F., Glass B. P., Hecht L., Mader D., and Reimold W. U. 2007a. Uppermost impact fallback layer in the Bosumtwi crater (Ghana): Mineralogy, geochemistry, and comparison with Ivory Coast tektites. *Meteoritics & Planetary Science* 42. This issue.

Koeberl C., Milkereit B., Overpeck J. T., Scholz C. A., Amoako P. Y. O., Boamah D., Danuor S., Karp T., Kueck J., Hecky R. E., King J. W., and Peck J. A. 2007b. An international and multidisciplinary drilling project into a young complex impact structure: The 2004 ICDP Bosumtwi Crater Drilling Project—An overview. *Meteoritics & Planetary Science* 42. This issue.

Leube A., Hirdes W., Mauer R., and Kesse G. O. 1990. The Early Proterozoic Birimian Supergroup of Ghana and some aspects of its associated gold mineralization. *Precambrian Research* 46: 139–165.

McCarville P. and Crossey L. J. 1996. Post-impact hydrothermal alteration of the Manson impact structure. In *The Manson impact structure, Iowa: Anatomy of an impact crater*, edited by Koeberl C. and Anderson R. R. GSA Special Paper #302. Boulder, Colorado: Geological Society of America. pp. 347–376.

Moore D. and Reynolds R. C. 1997. *X-ray diffraction and the identification and analysis of clay minerals*. New York: Oxford Press. 378 p.

Naumov M. V. 2002. Impact-generated hydrothermal systems: Data from Popigai, Kara, and Puchezh-Katunki impact structures. In *Impacts in Precambrian shields*, edited by Plado J. and Pesonen L. J. Berlin: Springer-Verlag. pp. 117–171.

Newsom H. E., Graup G., Sewards T., and Keil K. 1986. Fluidization and hydrothermal alteration of the suevite impact melt deposit at the Ries crater, West Germany, and implications for Mars. Proceedings, 17th Lunar and Planetary Science Conference. pp. E239–E251.

Newsom H. E., Graup G., Iseri D. A., Geissman J. W., and Keil K. 1990. The formation of the Ries crater, West Germany: Evidence of atmospheric interactions during a larger cratering event. In *Global catastrophes in Earth history: An interdisciplinary conference on impacts, volcanism, and mass mortality*, edited by Sharpton V. L. and Ward P. D. GSA Special Paper # 247. Boulder, Colorado: Geological Society of America. pp. 195–205.

Newsom H. E., Hagerty J. J., and Thorsos I. E. 2001. Location and sampling of aqueous and hydrothermal deposits in Martian impact craters. *Astrobiology* 1:71–88.

Newsom H. E., Nelson M. J., Shearer C. K., and Dressler B. O. 2006. Mobile element analysis by secondary ion mass spectrometry (SIMS) of impactite matrix samples from the Yaxcopoil-1 drill core in the Chicxulub impact crater. *Meteoritics & Planetary Science* 41:1929–1946.

Puura V., Huber H., Kirs J., Karki A., Suuroja K., Kirsimae K., Kivisilla J., Kleesment A., Konsa M., Preeden U., Suuroja S., and Koeberl C. 2004. Geology, petrography, shock petrography, and geochemistry of impactites and target rocks from the Kärdla crater, Estonia. *Meteoritics & Planetary Science* 39:425–451.

Schnetzler C. C., Pinson W. H., and Hurley P. M. 1966. Rubidium-strontium age of the Bosumtwi crater area, Ghana, compared with the age of the Ivory Coast tektites. *Science* 151:817–819.

Schnetzler C. C., Philpotts J. A., and Thomas H. H. 1967. Rare earth and barium abundances in Ivory Coast tektites and rocks from the Bosumtwi crater area, Ghana. *Geochimica et Cosmochimica Acta* 31:1987–1993.

Scholz C. A., Karp T., Brooks K. M., Milkereit B., Amoako P. Y. A., and Arko J. A. 2002. Pronounced central uplift identified in the Lake Bosumtwi impact structure, Ghana, using multichannel seismic reflection data. *Geology* 30:939–942.

Taylor P. N., Moorbath S., Leube A., and Hirdes W. 1992. Early Proterozoic crustal evolution in the Birimian of Ghana: constrains from geochronology and isotope geochemistry. *Precambrian Research* 56:97–111.

Tuchscherer M. G., Reimold W. U., Koeberl C., and Gibson R. L. 2005. Geochemical and petrographic characteristics of impactites and Cretaceous target rocks from the Yaxcopoil-1 borehole, Chicxulub impact structure, Mexico: Implications for target composition. *Meteoritics & Planetary Science* 40:1513–1536.

Walker J. R. 1987. Structural and compositional aspects of low-grade metamorphic chlorite. Ph.D. thesis, Dartmouth College, Hanover, New Hampshire, USA.

Walker J. R. 1993. Chlorite polytype geothermometry. *Clays and Clay Minerals* 41:260–267.